



Hybrid Effect of PVA Fibre and Carbon Nanotube on the Mechanical Properties and Microstructure of Geopolymers

Tao Meng^{1*}, Xiufen Yang¹, Yue Yu^{1,2}, Hongming Yu^{1,3} and Miaozhou Huang^{1,4}

¹College of Civil Engineering and Architecture, Zhejiang University, Hangzhou, China, ²Urban Planning and Architectural Design Institute of Fudan University Co., Ltd, Hangzhou, China, ³Hangzhou Xincheng Dinghong Real Estate Development Co., Ltd, Hangzhou, China, ⁴Wenzhou Design Assembly Company Ltd., Wenzhou, China

OPEN ACCESS

Edited by:

Cristina Leonelli,
University of Modena and Reggio
Emilia, Italy

Reviewed by:

Ruy Alexandre Sá Ribeiro,
National Institute of Amazonian
Research (INPA), Brazil
Jian Huang,
Wuhan University of Technology,
China

*Correspondence:

Tao Meng
taomeng@zju.edu.cn

Specialty section:

This article was submitted to
Structural Materials,
a section of the journal
Frontiers in Materials

Received: 09 September 2021

Accepted: 08 November 2021

Published: 25 November 2021

Citation:

Meng T, Yang X, Yu Y, Yu H and
Huang M (2021) Hybrid Effect of PVA
Fibre and Carbon Nanotube on the
Mechanical Properties and
Microstructure of Geopolymers.
Front. Mater. 8:773103.
doi: 10.3389/fmats.2021.773103

The concept of geopolymers has been widely studied since it was proposed. However, the wide range of applications of geopolymers is affected by brittleness and poor crack resistance. In this study, the mechanical properties of geopolymers with single-doped PVA fibres, single-doped carbon nanotubes, and mixed PVA fibers and carbon nanotubes were studied respectively first. It was found that PVA fibres and carbon nanotubes had a positive effect on improving the mechanical properties of geopolymers, especially bending strength and flexural strength. Moreover, the incorporation of PVA fibre could improve the damage morphology of geopolymers. Additionally, the phase analysis, structural group analysis, and strengthening mechanism were studied via scanning electron microscopy, mercury intrusion porosimetry analysis, X-ray diffraction pattern characterisation, Fourier transform infrared spectroscopy analysis, and magic angle spinning nuclear magnetic resonance analysis. It was found that the strengthening effect of PVA fiber to the geopolymer was primarily a physical strengthening effect, whereas the strengthening effect of carbon nanotubes to the geopolymers was both chemical and physical. Finally, based on the previous study, a multi-scale dual-fibre strengthening mechanism was proposed. Micro-nano fibre composites were used to improve microstructure via physical and chemical effects. This is helpful to improve the performance and application of geopolymers. Furthermore, it lays a preliminary theoretical foundation for engineering applications and technical improvement of geopolymers in the future.

Keywords: strengthen, fibre, nanometer material, microscopic analysis, mechanical characteristics

INTRODUCTION

Research on geopolymers began in the 1930s and 1940s. Purdon (1940) used the reaction of slag and hydroxide to prepare a fast-setting high-strength cementing material and proposed the alkali catalysis mechanism. Davidovits et al. understood the polymerisation mechanism of mineral polymer materials while studying the use of silica-alumina materials to prepare fireproof building materials. In 1979, they proposed the concept of geopolymers (Davidovits et al., 1979). He pointed out that geopolymers are a new type of inorganic aluminosilicate cementitious material with a three-dimensional network structure similar to that of an organic polymer (Davidovits, 1998).

Geopolymers can be obtained from various raw materials and require less production energy (Shi et al., 2020). The energy consumption and CO₂ emission for the production of 1 ton of geopolymer is 41 and 20%, respectively, of that of ordinary Portland cement (Davidovits, 2013). Since 1978, the research and application of geopolymers have attracted the attention of scientific researchers worldwide. It has been used in digital construction, repair materials, fast hardening and early strength materials, high-temperature refractory materials, and high-strength structural materials (Nematollahi et al., 2019). The density of geopolymers, about 1.8 g/cm³, is similar to that of ceramics, with high strength and rapid strength development (Lizcano et al., 2012). The strength of geopolymers can reach over 100 MPa (Sá Ribeiro et al., 2017). Moreover, the hot pressing process can also improve the compressive strength of geopolymer. The flexural strength of a geopolymer with metal fibres can reach up to 350 MPa. Generally, geopolymers can attain more than 70% of the strength attained in 28 days within 24 h, and the strength attained in 3 days can be more than 90% of the strength attained in 28 days (Yaseri et al., 2017). However, the elastic modulus of geopolymers is only a quarter of that of ceramics. For example, by using a Na₂O/SiO₂/NaOH ratio of 1.6, samples showed elastic modulus of about 10 GPa (Pelissera et al., 2013). On the other hand, the physical property of geopolymer is also influenced by its chemical structure (Li et al., 2020). Because of the unique cage structure (Davidovits et al., 1990; Davidovits, 1994a), geopolymers can effectively consolidate heavy metal ions. Moreover, it can be used as a thin-film adsorption material to seal heavy metal ions and radioactive elements.

In addition to high strength and good heavy metal ion consolidation, many studies have shown that geopolymers have good acid and alkali corrosion resistance, fire resistance, and high-temperature resistance. After soaking in 5% sulphuric acid solution and hydrochloric acid solution separately for 30 days respectively, the mass loss rate of the geopolymer was stable at 5–8% compared to that of traditional cement at 70–95% (Davidovits, 1994b). In a high-temperature environment, owing to the presence of highly distributed nanopores in the ceramic-like microstructure of geopolymers, free water and bonding water are allowed to migrate without destroying the three-dimensional network-like bonding structure of the geopolymer (Duxson, 2007), thereby reducing the negative impact of the high-temperature environment. Kong et al. (2007) found that the strength of fly ash-based geopolymers increased by 6% after being burned at a high temperature of 800°C.

Although geopolymers have many excellent mechanical and durability properties, they are brittle with insufficient toughness. When subjected to external forces, they tend to fracture like ceramics, which is undesirable for engineering applications. To reduce the brittleness and improve the toughness of geopolymers, scholars have performed various studies on the strength, mechanism, and dynamic characteristics of fibre-reinforced geopolymers.

Fibre-reinforced geopolymers are similar to fibre-reinforced cement-based materials. Fibre-reinforced geopolymers are prepared by adding a certain amount of fibres to strengthen

and toughen the geopolymer matrix. He et al. (2016) and Yuan et al. (2016) studied the influence of SiC fibre content and fibre length on geopolymers. The test results showed that SiC fibre had significant strengthening and toughening effects. The toughening mechanism was the same as that of fibre toughening in cement-based materials, i.e., a weak interface bond formed by mechanical interlocking. Nematollahi et al. (2017) and Nematollahi et al. (2019) studied the influence of the fibre-matrix interface characteristics on the crack bridging of composite materials based on a micromechanical model of PVA short fibres and fly ash-based geopolymer to explain the macro-mechanical characteristics. Sukontasukkul et al. (2018) studied the effect of mixing steel fibres and PP fibres in different proportions on the bending properties of geopolymers. Khan et al. (2018) used a Hopkinson pressure bar device to study the dynamic compressive properties of steel fibre-PE fibre-reinforced geopolymers and compared them under quasi-static conditions. Based on the observation results, an empirical dynamic increase factor relationship was proposed to simulate geopolymer composite materials and structures under static and impact loads.

In addition to using conventional PVA fibres and steel fibres for geopolymer enhancement, carbon nanotubes (CNTs) have also been used in the study of strengthening geopolymers since they were first discovered in 1991 (Iijima, 1991). The axial tensile strength of CNT is high, whereas the axial Young's modulus is approximately 270–950 GPa (Yu et al., 2000b). However, CNTs are soft along the radial direction (Yu et al., 2000a; Yang and Li, 2011), i.e., it will not break when it is bent or twisted, but become flat at the bending part (Ruoff and Lorents, 1995). High strength and high toughness enables the fabrication of composite materials with high-strength and high-toughness.

Presently, the influence of CNT on geopolymers has been studied less because of mainly focusing on improving the mechanical and electrical properties of geopolymers. Kusak et al. (2016) incorporated CNTs into a fine-abrasive blast furnace slag-based geopolymer and found that the absolute value of impedance decreased with an increase in the amount of CNTs. Moreover, the relative dielectric constant increased overall. Hamzaoui et al. (2014) found that adding CNTs (0.01% by weight of cement) to the mortar could significantly improve the strength and rigidity of the mortar. Researcher also found that the best spatial distribution and crack propagation control of MWNTs in nanocomposites were observed with concentrated alkali activators, such as sodium silicate (Liebsche et al., 2017). Carriço et al. (2018) studied the effects of different types of MWNTs on the durability of concrete to prove that mixing different types of MWNTs could improve the mechanical properties and durability of each group of concrete with different water-cement ratios. Additionally, MWNTs played a role in crack bridging and nanometre nucleation effect. Saafi et al. (2013) found that adding MWNTs could improve the flexural strength, Young's modulus, and flexural toughness of fly ash-based geopolymers effectively, while enhancing the fracture energy of geopolymers. Khater and Gawaad (2016) studied the effects of MWNTs on the mechanical properties and microstructure of slag-based geopolymers and found that 0.1wt% and 0.4wt% of multi-walled CNTs can increase the

TABLE 1 | Chemical composition of metakaolin and water glass.

Oxide composition	Al ₂ O ₃ (%)	SiO ₂ (%)	Na ₂ O (%)	H ₂ O (%)	Others (%)
Metakaolin	32.60	59.72	0.00	0.00	7.68
Water glass	0.00	27.35	8.42	64.23	0.00

strength of geopolymers. Rovnanik et al. (2016a, 2016b) found that as the content of MWNCTs increased, the basic fracture parameters (fracture toughness and fracture energy) of fly ash-based and slag-based geopolymers decreased initially and then recovered or increased slightly. Yang et al. (2017) incorporated CNT strengthened with PI fibres into phosphoric acid-based geopolymers and proved that CNTs strengthened with PI fibres could increase the compressive strength of geopolymers and improve their fracture properties. Yuan et al. (2017) found that the flexural strength, elastic modulus, and fracture toughness of multi-walled CNT-reinforced geopolymers improved significantly after high-temperature treatment at 950–1200°C.

In summary, steel fibres and carbon fibres are usually used to strengthen and toughen geopolymers. There are few studies on the effect of CNT-strengthened geopolymers; however, there is insufficient research on their physical and mechanical properties. Nevertheless, research on the strengthening effect of the dual-fibre composite toughened geopolymer is also scarce; particularly, theoretical research on the strengthening mechanism still needs further exploration.

In this study, the strengthening effects of single-doped PVA fibres, single-doped CNTs, and mixed PVA fibres and CNTs on the mechanical properties of geopolymers were analysed. The bending strength, compressive strength, and flexural strength were studied separately. Scanning electron microscopy (SEM) and mercury intrusion porosimetry (MIP) analysis were used to study the microscopic morphology and pore structure of geopolymers, respectively. X-ray diffraction (XRD) pattern characterisation, Fourier transform infrared spectroscopy (FTIR) analysis, magic angle spinning-nuclear magnetic resonance analysis (MAS NMR), and other technical means were used to study the basic structural group, amorphous system, and the structure and dynamics of the system. Finally, based on the multi-scale microscopic analysis of the strengthening effect of geopolymers by PVA fibres and CNTs, a multi-scale dual-fibre strengthening mechanism was proposed.

MATERIALS AND METHODS

Raw Materials

The metakaolin used in this experiment was an industrial-grade product produced by BASF, Germany. The oxide contents are shown in **Table 1**. The alkali activator was composed of sodium water glass, solid NaOH, and water (tap water). The sodium water glass, which was obtained from Tongxiang Hengli Chemical Co., Ltd., has a modulus of 3.36, and the equivalent oxide content is shown in **Table 1**. The solid NaOH was a flake solid produced by Sinopharm Chemical Reagent Co., Ltd., with a purity of over 96.0%.

The water reducing agent (Na₂CO₃) used in this experiment was a white powder produced by Sinopharm Chemical Reagent Co., Ltd., with a purity of over 99.8%. The defoamer model used was AGITAN[®] P 803. The PVA fibres used in this study was an industrial-grade product produced by Nanjing Painier Technology Industrial Co., Ltd., and the parameters are listed in **Table 2**. The CNTs were industrial-grade multi-walled CNTs manufactured by Suzhou Tanfeng Graphene Technology Co., Ltd., and the performance parameters are listed in **Table 2**.

Mix Proportions and Curing Methods

Based on previous studies, 1‰ of defoamer and 3.3‰ of Na₂CO₃ (relative metakaolin mass ratio) were added to the basic mix proportions of SiO₂/Al₂O₃, Na₂O/Al₂O₃, and H₂O/Na₂O of 4.30, 0.95, and 12.63, respectively (Zhang and Yang, 2001; Wu and Zhang, 2017). The PVA fibre content was determined according to the recommendations provided by the manufacturer (Zhang et al., 2019). The test arrangements for the single-doped CNTs and single-doped PVA fibres are shown in **Table 3**.

In the mixed group, based on the test results of the single-doped group, the best bending strength of the PVA fibre-strengthened geopolymer and CNT-strengthened geopolymer along with the content of both sides (1.2 kg/m³ and 1.5‰, respectively) were selected for the orthogonal test. Thus, groups P1, P2, P3, T3, T4, and T5 were selected. The test contents are listed in **Table 3**. In this experiment, the bulk density of the geopolymer was 1.78 g/cm³.

In this experiment, CNTs were first added to the prepared alkali activator solution and stirred uniformly without precipitation for some time before preparing the CNT-strengthened geopolymers. Metakaolin was mixed evenly with a water-reducing agent and defoamer before adding PVA fibres. This mixture was then mixed with an alkali activator solution, which was mixed with CNTs. Finally, the fresh mixture was poured into the corresponding mould, demolded after 24 h, and placed in a curing room maintained at a temperature of 20 ± 2°C and relative humidity of more than 95% for curing.

Testing Methods

Mechanical Properties

The mechanical properties of geopolymers, such as bending strength, compressive strength, and flexural strength, were tested according to the standard for test method of basic properties of construction mortar (China national standards, 2009).

The bending strength of the geopolymer specimens with dimensions of 40 mm × 40 mm × 160 mm, was tested using a 1000 N cement mortar testing machine. The loading speed was 10 N/s and the accuracy was 0.02 MPa. After the bending test, a compression test was performed on the two broken specimens.

TABLE 2 | Main performance parameters of PVA fibre and multi-walled CNTs.

Parameters	Value	Parameters	Value
PVA Fibre type	Bundle monofilament	PVA Fibre Length	6 mm
PVA Fibre Monofilament diameter	5–20 μm	PVA Fibre Elastic Modulus	32–40 GPa
PVA Fibre Tensile strength	1200–1500 MPa	PVA Fibre Elongation at break	5–15%
CNTs Purity	>95%	CNTs Length/ μm	3–12
CNTs Outer diameter (nm)	12.9 \pm 3.5	CNTs Aspect ratio (L/D)	230–930
CNTs Inner diameter (nm)	3–5	CNTs Specific surface area	>233 m^2/g
CNTs Wall thickness (nm)	4.1 \pm 1.3	CNTs Density	0.15 g/cm^3
Number of carbon Tube layers	8–15	CNTs Resistivity	100 s/cm

TABLE 3 | Single-doped PVA fibre, single-doped CNT, and mixed-doped strengthened geopolymer test group arrangement.

	No.	PVA (kg/m^3)	CNT%	
Single-doped group	B0	0	0	
	P1	0.9	0	
	P2	1.2	0	
	P3	1.5	0	
	P4	1.8	0	
	P5	2.1	0	
	T1	0	0.5	
	T2	0	0.8	
	T3	0	1.2	
	T4	0	1.5	
	T5	0	1.8	
	T6	0	2.1	
	Mixed group	B0	0	0
		PT1	0.9	1.2
		PT2	0.9	1.5
		PT3	0.9	1.8
PT4		1.2	1.2	
PT5		1.2	1.5	
PT6		1.2	1.8	
PT7		1.5	1.2	
PT8		1.5	1.5	
PT9		1.5	1.8	

The measuring range of the pressure testing machine was 100 kN, and the stress area was 40 mm \times 40 mm. In the experiment, the loading speed was maintained at 50 kN/min to ensure that the measurement process was quasi-static. The flexural strength of the geopolymer specimens, whose dimensions were 100 mm \times 100 mm \times 400 mm, was tested using a universal testing machine. The specimens were tested at 7 and 28 days old. The bending strength formula was:

$$f_f = \frac{Fl}{bh^2}$$

In the formula, f_f referred to bending strength (MPa), F referred to specimen failure load (N), l referred to span between supports and it was equal to 3 h (mm), b referred to section width of test piece (mm), h referred to section height of test piece (mm). The lower support span was 120 mm. The two loading points on the upper surface were at the trisection of the specimen span. The test value was the average of the three measured values.

The flexural strength formula was:

$$\sigma_f = \frac{3Fa}{bd^2}$$

In the formula, σ_f referred to flexural strength (MPa), F referred to specimen failure load (N), a referred to length of flexural force arm (mm), b referred to section width of test piece (mm), d referred to section height of test piece (mm). Four-point loading method was adopted. The test value was the average of the three measured values.

For sampling, after conducting the mechanical properties test, the tested specimen should be collected, broken into small samples with a particle size of 0.5–1 cm, and then placed in absolute ethanol to stop hydration. The samples were dried before the test and sealed in a double-layer sealing bag for use as SEM and MIP test materials. XRD, FTIR, and MAS NMR samples were prepared in the same manner as that for SEM, but before sealing, it was ground into a fine powder and passed through an 80 μm square-hole sieve.

XRD Analysis

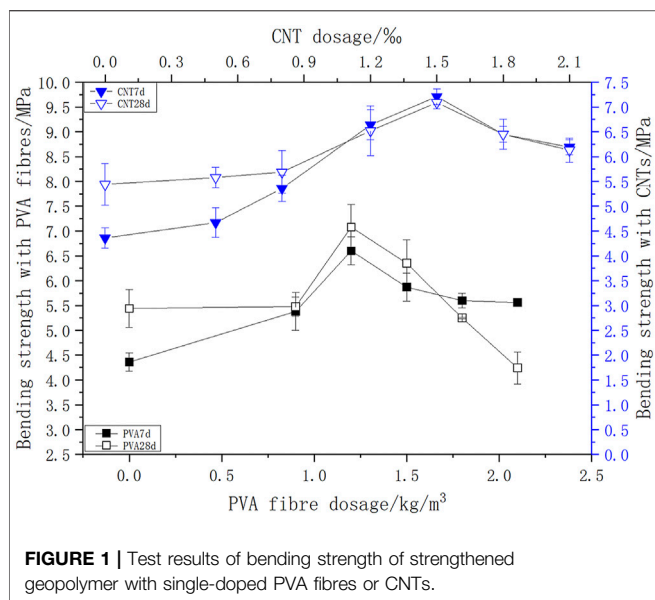
XRD was used to obtain the diffraction patterns of the materials. According to the patterns, the composition of materials and the structure or morphology of atoms or molecules in the materials were analysed. In this experiment, the X-ray diffractometer (PANalytical, the Netherlands) in the XRD Microscopic Laboratory of the School of Materials at the Zhejiang University was used.

FTIR Spectroscopy Analysis

Infrared light irradiation can cause chemical bonds or functional groups of the materials to vibrate and absorb to form an infrared spectrum. According to the infrared spectrum, the structural groups of the materials can be analysed qualitatively. In this experiment, the FTIR test was performed using the Agilent 6890-Nicolet 5700 pyrolysis gas chromatography-infrared spectrometer in the State Key Laboratory of Chemical Engineering, Zhejiang University. The infrared interferometer was a Vectra-Plus interferometer.

MAS NMR Analysis

MAS NMR uses the transition of the atomic nucleus of an atom under the action of an external magnetic field to form the nuclear magnetic resonance spectrum. According to the nuclear magnetic resonance spectrum, the structure and dynamics of the material can be analysed. In this experiment, the Avance III HD solid-state



nuclear magnetic resonance spectrometer at the Institute of Physical Chemistry was used for the MAS NMR test to analyse the ^{29}Si and ^{27}Al magic angle rotating nuclear magnetic resonance spectroscopy of the geopolymer samples.

SEM Analysis

By observing the surface of the sample, the compactness, composition, micromorphology, and products of the material can be analysed. In this experiment, the SEM test was performed using an FEG-650 field emission environmental scanning electron microscope and an energy spectrometer from the School of Civil Engineering and Architecture, Zhejiang University.

MIP Analysis

Mercury can be pressed into the microporous material only under an external force. Therefore, the pore structure of the material can be analysed by measuring the amount of mercury entering under different external pressures. In this experiment, an AutoPore IV9510 automatic mercury porosimeter was used in the MIP test.

EFFECTS OF PVA FIBRES AND CNTS ON THE MECHANICAL PROPERTIES OF GEOPOLYMER

Geopolymer Strengthened by Single-Doped PVA Fibre or CNT

Results and Discussions on Bending Strength

The bending strength test results of the PVA fibre-strengthened geopolymer and CNT-strengthened geopolymer are shown in Figure 1.

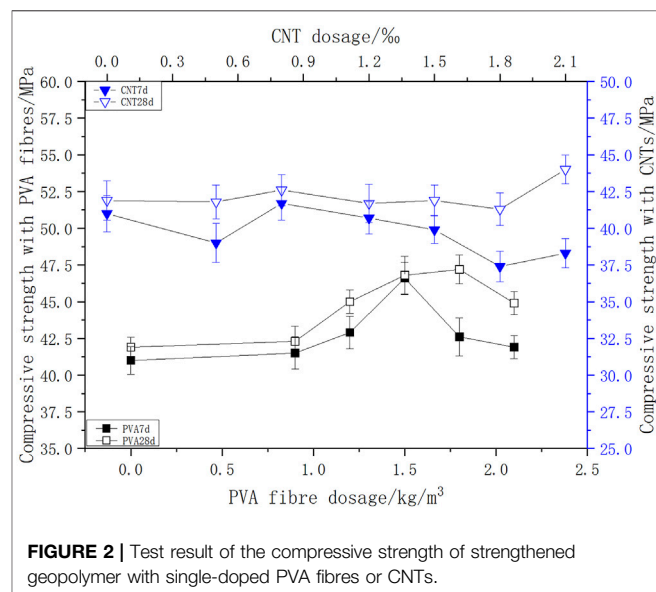
It was found that the 7-day bending strength of geopolymers was more than 80% of the 28-day bending strength with some geopolymers attaining more than 95% of the bending strength.

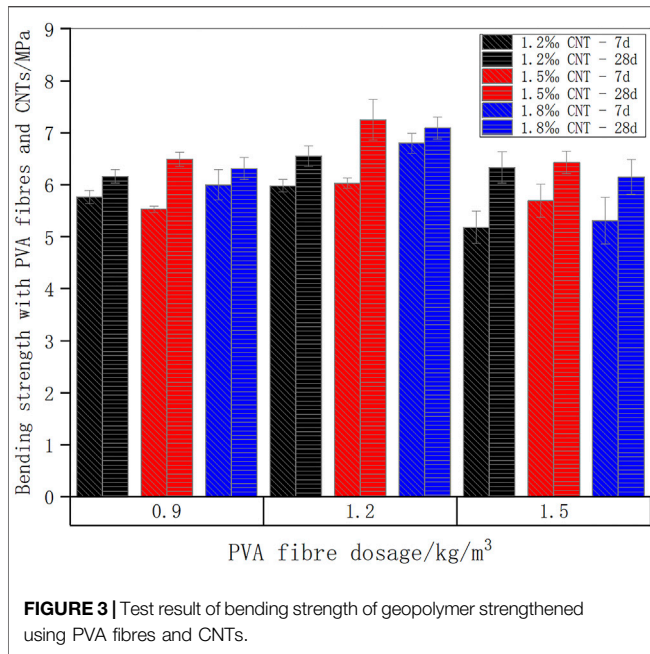
Figure 1 shows that the bending strength of geopolymers mixed with PVA fibres or CNTs increased with an increase in the content and then decreased. This indicates that although PVA fibres and CNTs can improve the bending strength of geopolymers, but it's not that the more the better. The optimal volume of PVA fibre was 1.2 kg/m^3 (P2 group). Compared with the B0 group (without PVA fibres), the 7-day bending strength was increased by 51.4%, whereas the 28-day bending strength increased by 30.1%. As the volume of PVA fibres continued to increase (P3, P4, and P5 groups), the bending strength of the PVA fibre-strengthened geopolymers gradually decreased relative to that of the P2 group. This might be due to the limitation of the moulding process, i.e., the fibres cannot be well dispersed and result in fibre aggregation, which makes the strengthening role cannot be effectively played. Thus, cracks form and expand rapidly in these areas, leading to the fracture of the specimen.

The optimal CNT content was 1.5‰ (the mass ratio relative to the content of metakaolin, T4 group). Compared with the B0 group without CNT, the 7-day and 28-day bending strengths increased by 65.4 and 30.3%, respectively. When the CNT content was between 0.5 and 1.5‰, the bending strength of the geopolymer was enhanced significantly. The 28-day bending strength of the geopolymer increased almost linearly. When the CNT content was between 1.5 and 2.1‰, the 28-day bending strength of the geopolymer decreased gradually. This may be because CNT could give full play to micro-filling, mechanical interlocking, and other functions when the CNT content was appropriate. However, when the CNT content is too high, there may be weak areas in the structure because CNT cannot be well dispersed. Thus, CNT cannot play a good role.

Results and Discussions on Compressive Strength

The compressive strength test results of the PVA fibre-strengthened geopolymer and CNT-strengthened geopolymer are shown in Figure 2.





The compressive strength of the geopolymer was found to be similar to the bending strength. The 7-day strength of the specimens could reach more than 85% of the 28-day strength in the single-doped group. Moreover, some specimens could reach more than 95% of the 28-day strength. However, the strength shrinkage phenomenon was not observed. This indicated that the strength shrinkage did not have a knock-on effect, and the reduction in the bending strength did not mean that the compressive strength was also reduced. The 7-day compressive strength of mixed PVA fibres and CNTs could reach more than 90% of the 28-day strength, and there were very few cases of strength shrinkage, such as the PT3 and PT9 groups.

Figure 2 indicates that the compressive strength of geopolymers increased initially with an increase in PVA fibre content and then decreased. The effect of CNTs on the compressive strength of the geopolymer was not very obvious. In the experiment related to PVA fibre-strengthened geopolymer, the P3 group had the highest 7-day compressive strength, which was 13.7% higher than that of the B0 group (without PVA fibre and CNT). The P4 group had the highest 28-day compressive strength, which was 12.6% higher than that of the B0 group. As for geopolymer strengthened with CNTs, the T2 group had the highest 7-day compressive strength (41.7 MPa), which was 0.5% lower than that of the B0 group. The T6 group had the highest 28-day compressive strength (44.0 MPa), which was 5.0% higher than that of the B0 group. CNTs had little effect on the compressive strength of the geopolymer. Except for the T6 and T2 groups, the 28-day compressive strength of other groups was almost the same as that of the B0 group.

Geopolymer Strengthened With PVA Fibres and CNTs

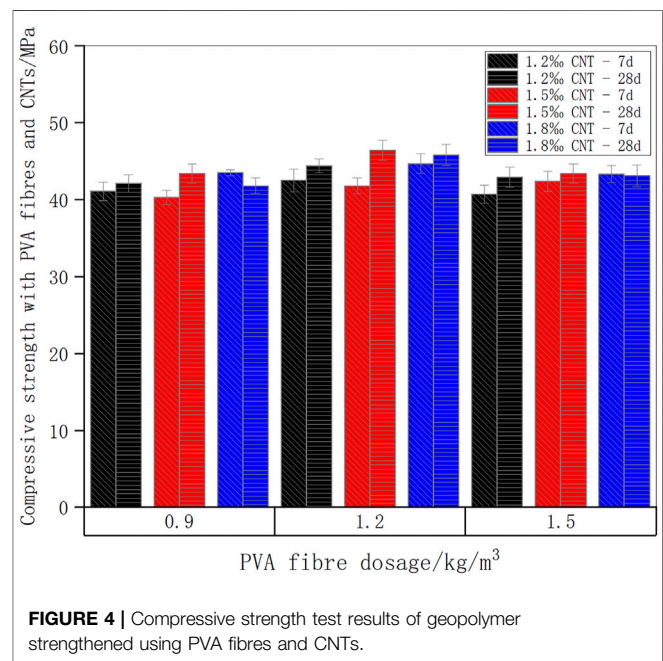
Results and Discussions on Bending Strength

The bending strength test results of geopolymers strengthened using PVA fibres and CNTs are shown in Figure 3.

From Figure 3, it can be observed that compared with the group B0 (without PVA fibre and CNT), the 7-day bending strength of geopolymers strengthened by both PVA fibres and CNTs increased by 33.2% on average. The 7-day bending strength of the PT6 group was the highest (6.80 MPa), which increased by 56.0%. The 28-day bending strength increased by 20.0% on average. The PT5 group had the highest 28-day bending strength (7.25 MPa), which increased by 33.3%.

When the volume of PVA fibres was 0.9 kg/m^3 with an increase in the CNT content, the 7-day bending strength of the geopolymer decreased initially and then increased. When the volume was 1.2 kg/m^3 , the 7-day bending strength increased as the CNT content increased continuously. When the volume content was 1.5 kg/m^3 , the 7-day bending strength first increased and then decreased with an increase in the CNT content. When the CNT content was 1.2, 1.5, and 1.8%, the 7-day bending strength first increased and then decreased with an increase in the PVA fibre content. This shows that when the curing age of the geopolymer was 7 days, the effect of CNTs on the blending of PVA fibres and CNT-strengthened geopolymers was not very obvious, while the effect of PVA fibres on it was more obvious.

When the geopolymer curing age reached 28 days, it was found that when the volume of PVA fibre content was 0.9, 1.2, and 1.5 kg/m^3 , the bending strength of the geopolymer increased initially with an increase in the CNT content and then decreased. However, when the CNT content was 1.2, 1.5, and 1.8%, the bending strength of the geopolymer increased



initially and then decreased with the increase in the volume of PVA fibre. This shows that when the geopolymer curing age reached 28 days, the strengthening effect of PVA fibres and CNTs on the geopolymer was very obvious.

Results and Discussions on Compressive Strength

The compressive strength test results of geopolymers strengthened using PVA fibres and CNTs are shown in **Figure 4**.

Figure 4 shows that not all the compressive strength of the geopolymer strengthened with PVA fibres and CNTs improved. The 7-day compressive strength of the PT2 and PT7 groups and the 28-day compressive strength of the PT3 group decreased in varying degrees. The PT6 group had the highest 7-day compressive strength (44.7 MPa), which was 9.0% higher than that of the B0 group. The PT5 group had the highest 28-day compressive strength (46.4 MPa), which was 10.7% higher than that of the B0 group.

When the volume content of PVA fibres were 0.9 and 1.2 kg/m³, the 7-day compressive strength of the geopolymer decreased first and then increased with the increase in the CNT content. When the volume content of PVA fibres was 1.5 kg/m³, the 7-day compressive strength increased with an increase in the CNT content. When the CNT content was 1.2 and 1.8‰, the compressive strength for 7 days increased initially and then decreased with an increase in the PVA fibre content. When the CNT content was 1.5‰, the 7-day compressive strength increased with an increase in the volume of PVA fibre.

When the geopolymer curing age reached 28 days, it was found that when the volume of PVA fibre content was 0.9, 1.2, and 1.5 kg/m³, the compressive strength of the geopolymer first increased and then decreased with an increase in the CNT content. When the CNT content was 1.2, 1.5, and 1.8‰, the compressive strength of the geopolymer first increased and then decreased with an increase in the volume of the PVA fibre. This shows that when the geopolymer curing age reached 28 days, the strengthening effect of PVA fibres and CNTs on the geopolymer was very obvious.

Results and Discussions on Flexural Strength

The groups B0, P2, T4, and PT5 were selected to prepare the flexural strength test samples. After the test, the flexural strength of B0 group turned out to be 6.45 MPa, while the value for P2 group, T4 group and PT5 group were 7.20, 7.35 and 7.80 MPa, respectively.

The results show that both single-doped and mixed-doped PVA fibres and CNTs can improve the flexural strength of the geopolymer. Compared with the B0 group, the flexural strength of the P2 group with 1.2 kg/m³ PVA fibre increased by 11.6%, T4 group with 1.5‰ CNTs increased by 14.0%, and PT5 group with PVA fibres and CNTs increased by 20.9%. The results showed that PVA fibres and CNTs can improve the flexural strength of geopolymers, and the improvement effect of CNTs was more significant than that of PVA fibres. Moreover, the flexural strength of geopolymers strengthened with PVA fibres and CNT was better than that of geopolymers strengthened with PVA fibres or CNTs. This shows that the combination of these two fibres had a good hybrid effect on the geopolymer.

Discussions on Damage Patterns

The damage morphology of the compressive strength test of the single-doped and mixed-doped PVA fibre and CNT-strengthened geopolymer are shown in **Figure 5**, respectively.

When PVA fibres were incorporated, the failure morphology of the geopolymer compression test specimens underwent significant changes. **Figure 5** shows the failure morphology of the geopolymer compression test with and without PVA fibres. This might be because the blended fibre played the role of crack bridging. The fibres close to the crack tip did not break, but the two ends of the crack were bridged to connect the two ends. A large number of fibres work together to change the damage morphology of the geopolymer. CNT had little effect on the damage morphology in the geopolymer compression test. This may be related to the low elongation rate of CNTs.

The damage morphology in the compressive strength test of the geopolymer strengthened with PVA fibres and CNTs was the same as that of the geopolymer strengthened with PVA fibres. This indicates that PVA fibres could effectively change the failure mode of geopolymers in the case of blending.

ANALYSIS OF THE RESULTS OF THE GEOPOLYMER MICROSCOPIC TEST

Geopolymer Phase Composition and Structural Group Analysis

Phase analysis—XRD Result Analysis

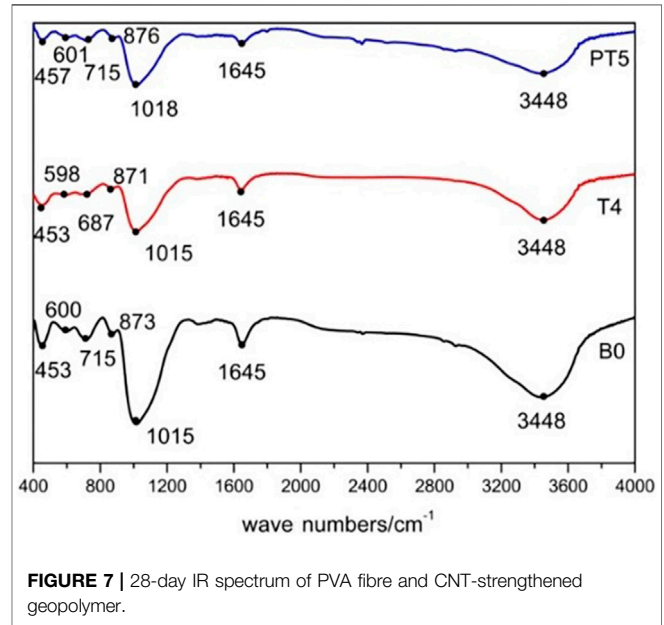
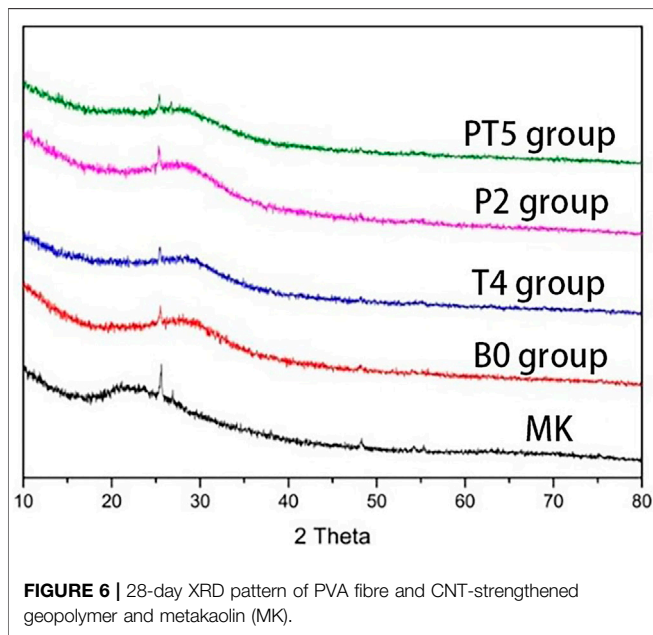
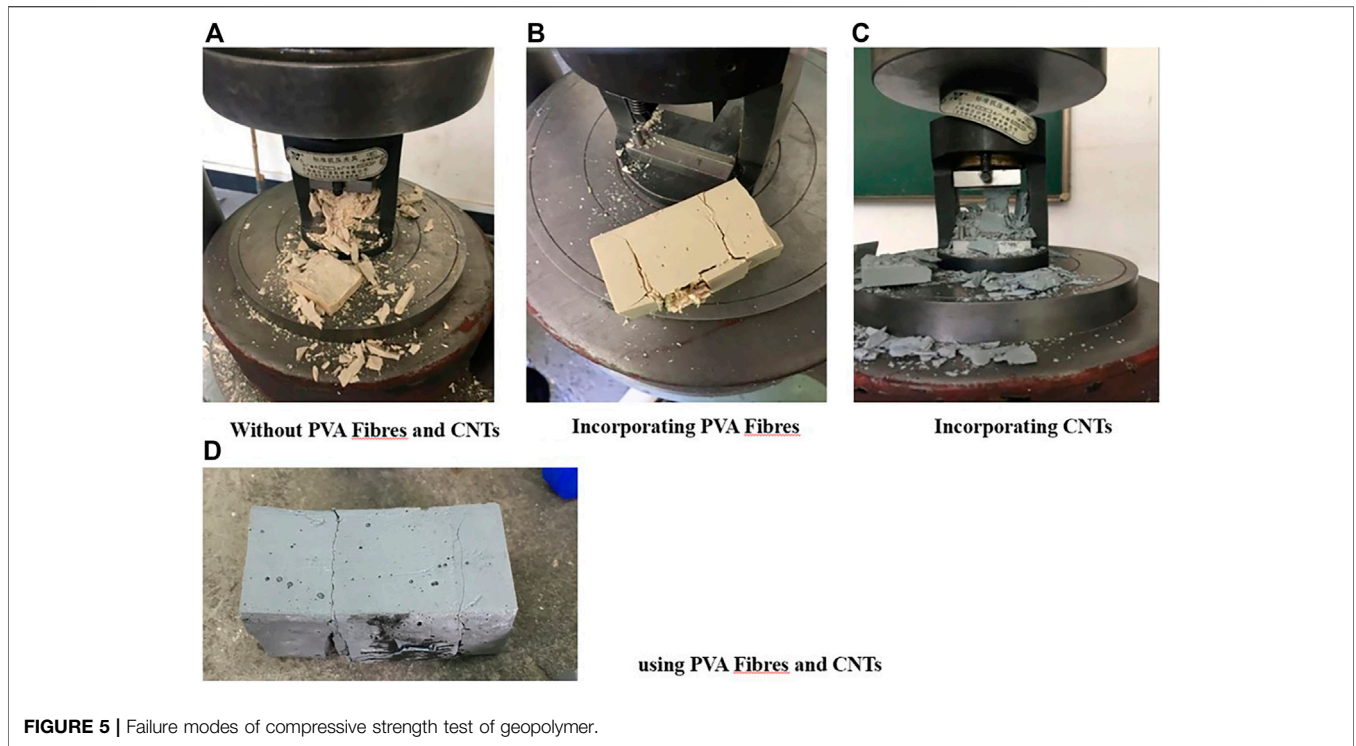
Figure 6 shows the 28-day XRD patterns of metakaolin, B0, T4, P2, and PT5 groups.

The map **Figure 6** shows that the reaction product of the PVA fibre and CNT-strengthened geopolymer was still primarily an amorphous material and the phase composition of the final product did not change. The sharp peak with a 2θ value of 25.580° in metakaolin moved left to 25.492° in the B0 and P2 groups and to 25.448° in the T4 and PT5 groups. The sharp characteristic peak corresponding to quartz in metakaolin disappeared after the reaction. Furthermore, after the geopolymer reaction, the broad dispersive peak at 17°–30° in metakaolin transformed to an 18°–38° diffused steamed bun-shaped peak. The steamed bun peaks observed in the T4 and PT5 groups were gentler than those in the B0 and P2 groups. This showed that metakaolin and quartz crystals in metakaolin participated in the geopolymerisation reaction to generate new substances. Compared with the B0 and P2 groups, the T4 and PT5 groups had a better amorphous structure. We speculated that CNTs could optimise the amorphous structure of the geopolymer to a certain extent.

Structural Group analysis—FTIR Analysis

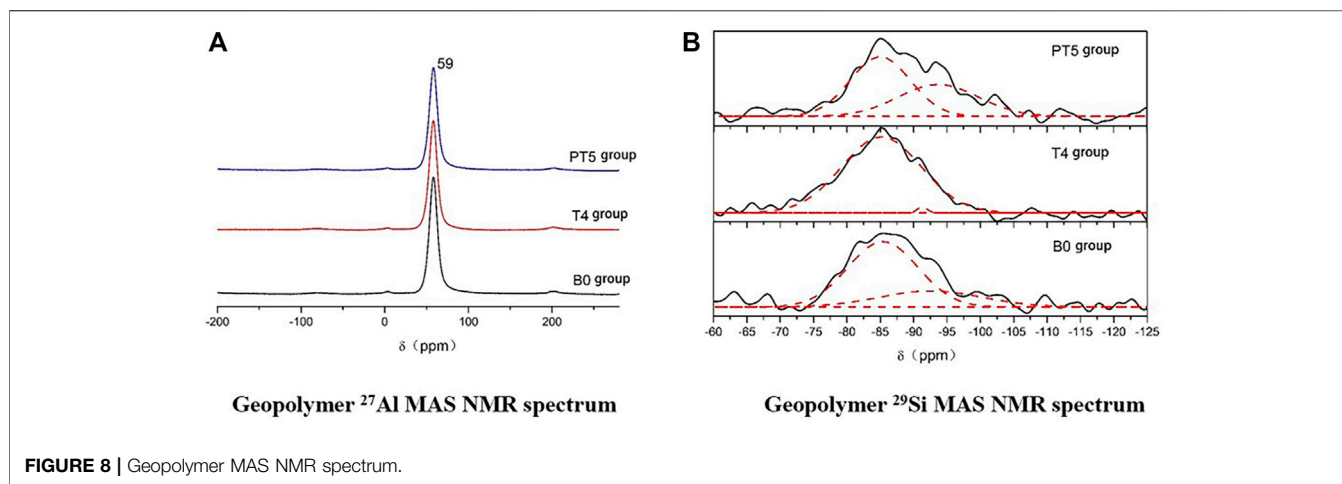
Figure 7 shows the infrared spectrum lines of the B0, T4, and PT5 groups.

Figure 7 indicates that the characteristic bands of single-doped CNTs and mixed-strengthened geopolymers are the same as those of unstrengthened geopolymers. Generally, the wave number corresponding to the asymmetric stretching vibration peak of the T—O—Si (T = Si or Al) bond moved toward the low-



frequency direction, i.e., more tetrahedral aluminium atoms replaced tetrahedral silicon atoms, thereby decreasing the compressive strength. The wave numbers of this peak (which peak) in groups B0, T4, and PT5 were 1,015 cm⁻¹, 1,015 cm⁻¹, and 1,018 cm⁻¹, respectively. These values accord with the test results that the 28-day compressive strength of the T4 group was the same as that of the B0 group, and the 28-day compressive

strength of the PT5 group was slightly higher than that of the B0 group. As the vibration area of the T4 and PT5 groups was significantly narrower than that of the B0 group in the wavenumber range of 900⁻¹–1,300 cm⁻¹, it was believed that the final product of the geopolymerisation reaction of the T4 and PT5 groups was more uniform with higher bending strength. The broad bands with wave numbers of 1,645 cm⁻¹ and 3448 cm⁻¹ were O-H bonds weakly bound to geopolymer



units and some H-O-H groups existing in the cavity of the three-dimensional network structure of the geopolymer. The vibration region of the T4 and PT5 groups at this wave number was narrower than that of the B0 group, indicating that more free water in the structure resulted in T4 and PT5 groups having higher bending strength.

By analysing the IR spectrum, no obvious vibration peak of the C-O bond or -COOH group was found in the spectral line after doping with CNTs to prove that the active part of CNTs was combined with the geopolymer structure and making CNTs a part of the geopolymer structure. Therefore, MAS NMR technology should be used in further analyses.

Analysis of the Degree of Geopolymer Micro-Polymerisation

The ^{27}Al MAS NMR and ^{29}Si MAS NMR spectral analyses of the geopolymers are shown in **Figure 8**.

Geopolymer ^{27}Al MAS NMR spectrum shows that the addition of CNTs and PVA fibres had no effect on the chemical shift δ corresponding to the characteristic peak of Al in the geopolymer. However, the ^{27}Al MAS NMR of the geopolymer had a characteristic peak. The shift was approximately 59 ppm, which corresponded to the 4-coordinate Al. According to the previous research, the extremely narrow peak at 59 ppm indicated that Al was present in the form of $\text{AlQ}_4(4\text{Si})$. Moreover, there were no low-molecular-weight dimers or trimers in the geopolymer. Geopolymers are a type of silicon aluminium compound with a three-dimensional network structure. Geopolymer ^{29}Si MAS NMR spectrum shows that the ^{29}Si MAS NMR spectrum of the Na-PSS geopolymer had a diffused peak at -85 ppm, indicating that the structure of the geopolymer was amorphous. Moreover, with the incorporation of CNTs, the peak shape at -85 ppm increased gradually. This might be because the incorporation of CNTs affected the structure of the geopolymer to a certain extent, indicating that there was a certain chemical reaction when CNTs strengthened the geopolymer. It is possible that a small number of active groups of CNTs participated in the geopolymer reaction

during the curing stage of the geopolymer. Simultaneously, the chemical shifts of the characteristic peaks were -85 and -91 ppm, which indicated that the bonding forms of Si in the Na-PSS geopolymer were $\text{Q}_4(3\text{Al})$ and $\text{Q}_4(2\text{Al})$. However, $\text{Q}_4(3\text{Al})$ was the main one.

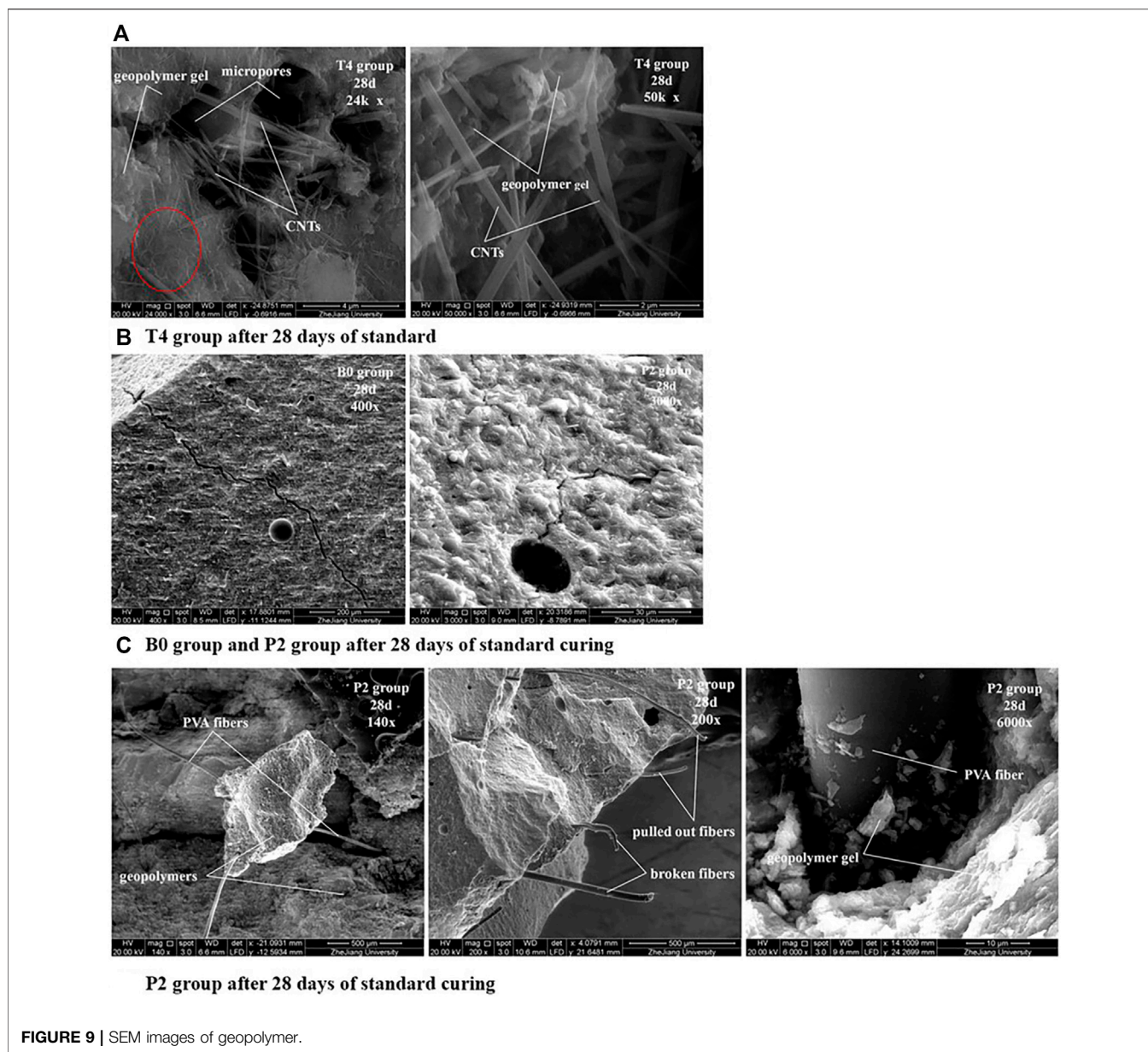
Analysis of the Microscopic Morphology and Pore Structure of Geopolymers

Microscopic Morphology Analysis—SEM Result Analysis

The SEM images of geopolymer are shown in **Figure 9**.

Figure 9A shows that the CNTs were evenly distributed in the geopolymer gel on the microscopic fracture surface of the geopolymer, and the agglomeration phenomenon was not observed. The CNT surfaces were relatively smooth. It was speculated that the improvement of geopolymer properties by CNTs was mainly because of the mechanical interlocking of the interface between the CNTs and the geopolymer matrix. Additionally, it could be observed that the CNTs bridged the two ends of the opening of the micropores. Some CNTs had one end in the geopolymer gel and the other end was damaged, which might have been caused by an external force. Therefore, in terms of the principle of strengthened geopolymers, it was believed that on one hand, CNTs played the role of micro-filling, i.e., connecting with each other in the micropores of the geopolymer, forming network like filling, and refining micropores. On the other hand, it played a bridging role. When the geopolymer was subjected to an external force, owing to the bridging effect of CNTs, additional work was needed to destroy the matrix. Therefore, it improved the mechanical properties of the matrix. In **Figure 9A**, it can be observed that some CNTs were wrapped by the geopolymer gel, thereby obtaining a larger bonding interface.

Figure 9B shows the scanning electron micrographs of the B0 group geopolymer at 400 \times magnification and the P2 group geopolymer at 3000 \times magnification after 28 days of standard curing. The figure shows that the cracks produced by the B0



group after being subjected to an external force were single cracks, while the cracks produced by the P2 group mixed with PVA fibres under the action of external force were deflected and bifurcated. This might be because the incorporation of fibres disrupts the original stress distribution inside the geopolymer matrix. When the geopolymer cracked, the presence of the fibres blocked or deflected the crack. Thus, additional work was needed to overcome the destruction of the matrix. In other words, it improved the shear stress bearing capacity of the matrix. Furthermore, it showed the improvement in macro mechanical properties and change in the failure mode of the compressive strength test.

Figure 9C shows that the fibre distribution in the geopolymer matrix was relatively uniform with no agglomeration. The fibres were bridged between two separate

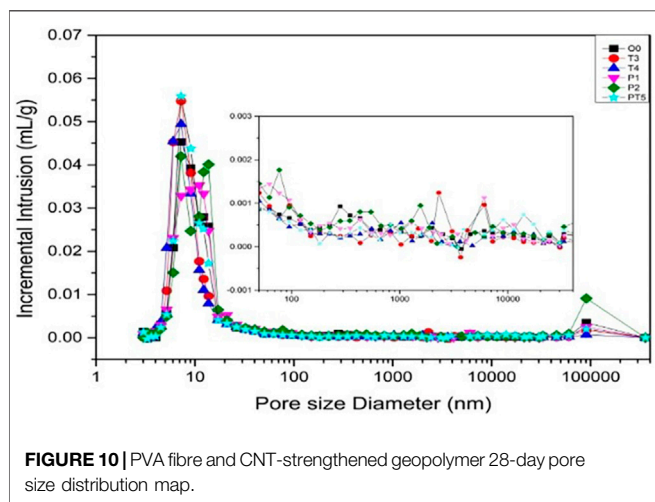
pieces of geopolymers. When the matrix was subjected to external forces, the fibres were pulled out and broken. Owing to the tight bonding between the fibre and geopolymer gel, the friction shear stress was high. The presence of fibres hinders crack development and induces deflection and bifurcation. Moreover, during crack propagation, the friction shear stress at the interface between the fibre and matrix should also be overcome. Therefore, the incorporation of fibres could improve not only the toughness of the geopolymer, but also the mechanical properties, and change the failure mode in compression tests.

Pore Structure Analysis—MIP Results Analysis

The MIP results of PVA fibre and CNT-strengthened geopolymer are shown in Table 4.

TABLE 4 | PVA fibre and CNT-strengthened geopolymer 28-day pore size distribution, percentage (ml/g) and Characteristic parameters of the pore structure.

	Group	B0	T3	T4	P1	P2	PT5
Characteristic parameters	Average pore size (nm)	10.6	9.1	8.6	10.7	11.7	10.2
	Total porosity (ml/g)	0.227	0.223	0.215	0.232	0.244	0.228
	Porosity (%)	31.96	31.77	30.95	32.30	33.28	32.00
pore size distribution and percentage	>200 nm distributed (percentage)	0.012 (5.5%)	0.009 (4.0%)	0.007 (3.3%)	0.012 (5.1%)	0.021 (8.5%)	0.012 (5.3%)
	50–200 nm distributed (percentage)	0.004 (1.6%)	0.004 (1.8%)	0.003 (1.4%)	0.005 (2.2%)	0.005 (2.2%)	0.004 (1.8%)
	20–50 nm distributed (percentage)	0.010 (4.5%)	0.010 (4.5%)	0.009 (4.2%)	0.014 (6.0%)	0.012 (5.0%)	0.010 (4.4%)
	< 20 nm distributed (percentage)	0.201 (88.5%)	0.200 (89.7%)	0.196 (91.2%)	0.202 (86.9%)	0.205 (84.0%)	0.201 (88.5%)

**FIGURE 10** | PVA fibre and CNT-strengthened geopolymer 28-day pore size distribution map.

Characteristic Parameters of Pore Structure

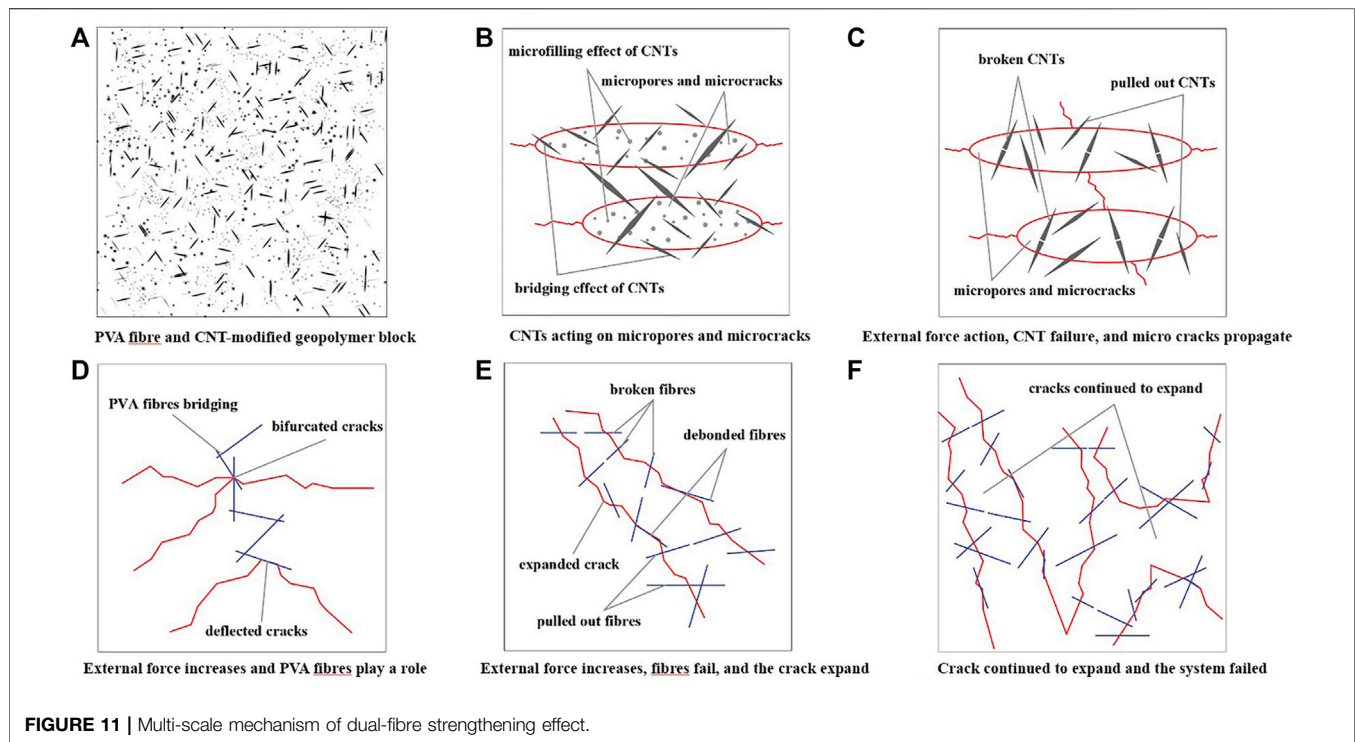
The test results showed that the incorporation of CNTs could help to improve the pore structure of the geopolymer, whereas the incorporation of PVA fibres might have an adverse effect on the pore structure of the geopolymer. Compared with the B0 group (without CNTs), the average pore size, total pore volume, and porosity of the T3 group with 1.2% CNTs decreased by 14.2, 1.8, and 5.9%, respectively, whereas that of the T4 group with 1.5% CNTs decreased by 18.9, 5.3, and 3.2%, respectively. Compared with B0 group, the average pore size, total pore volume, and porosity of the P1 group with PVA fibre volume content of 0.9 kg/m³ increased by 0.9, 2.2, and 3.2%, respectively, and the increase range increased with the increase in PVA fibre volume content. The average pore size, total pore volume, and porosity of the PT5 group with 1.5% CNTs and 1.2 kg/m³ PVA fibres increased compared with the T4 group with the same amount of CNTs, but decreased compared with the P2 group with the same amount of PVA fibres. The results showed that CNTs could play a micro-filling role, reduce the average pore size, total pore volume, and porosity, and form a more compact structure. When PVA fibres were added, the average pore size, total pore volume, and porosity of the geopolymer increased owing to the high viscosity of the geopolymer, which made it difficult to vibrate out the bubbles introduced by the fibres during the mixing process.

Pore Size Distribution

The relationship between pore size and mercury intake increase was drawn according to the results of the mercury intrusion test (Figure 10).

From Table 4, it can be observed that the pores of geopolymers doped with CNTs or PVA fibres are dominated by nanoscale gel pores, and harmless pores with a pore diameter of less than 20 nm account for more than 80%. By comparing the B0, T3, and T4 groups, it was found that the number of harmless pores with a pore diameter of less than 20 nm in the geopolymer incorporated with CNTs decreased while their proportion increased. By comparing the B0, P1, and P2 groups, it can be seen that the incorporation of PVA fibres increased the number of harmless pores in the geopolymer, while their proportion decreased and the number of capillary pores increased significantly. Compared with the T4 group, the number of harmless pores in the PT5 group increased and their proportion decreased. Compared with the P2 group, the number of harmless pores in the PT5 group decreased and their proportion increased. This showed that CNTs could exert their size effect by filling the pores in the geopolymer microstructure, refining the pore structure of the geopolymer, and forming a denser pore structure, thereby improving the macromechanical properties of the geopolymer. PVA fibres might cause more air bubbles in the geopolymer during the stirring process, thereby causing the capillary pores to increase. Moreover, the pore structure was looser than that of geopolymers without PVA fibres. Therefore, PVA fibres in geopolymers mainly improve the mechanical properties of geopolymers by mechanical interlocking rather than by participating in the reaction or improving the microstructure of the geopolymer.

The most probable pore sizes of groups B0, T3, and T4 were 11.0, 8.9, and 8.4 nm, respectively. The pore size distribution of groups T3 and T4 was narrower than that of group B0. The most probable pore sizes of P1 and P2 groups were 11.5 and 12.3 nm, respectively, and the distribution range of the pore size was wider than that of B0 group. The pore size distribution of the PT5 group was similar to that of the T3 and T4 groups, but the most probable pore sizes was slightly larger (10.2 nm). Compared with P1 and P2 groups, the pore size distribution of the PT5 group was narrower. This further showed that the



incorporation of CNTs into the geopolymer could play the role of micro-filling of CNTs, which helped to optimise the pore structure of the geopolymer and improved the macro mechanical properties of the geopolymer. However, PVA fibres did not improve the pore structure of the geopolymer. It was speculated that the improvement in the macromechanical properties of the geopolymer was mainly due to the physical effect. Some studies have also pointed out that there may be complexation reaction between PVA fibres and metal ions (Bonapasta et al., 2002). If the complexation reaction does exist, the strengthening performance of PVA fibres in the geopolymer may be further enhanced due to the chemical connection between PVA fibres and geopolymer matrix.

Multi-Scale Mechanism of Dual-Fibre Strengthening Effect

Based on the aforementioned test results, the geopolymer strengthening mechanism was analysed from the perspective of macrostructure and microstructure to propose the dual-fibre strengthening mechanism of PVA fibres and CNTs.

By studying the mechanical properties and microstructure of CNT-strengthened geopolymers, we found that the chemical strengthening effect of CNTs on geopolymers was manifested in the process of solidification of geopolymers and there may be some active groups involved. The reaction of the geopolymer forms a strong bond with the structure of the geopolymer, thereby optimising the crystal structure of the geopolymer.

Current research showed that the strengthening mechanisms of CNTs on geopolymers include:

- 1) Crack resistance: During the solidification process of the geopolymer, the condensation of the -OH group in the matrix and the evaporation of excess water in the macropores and pores caused the matrix to shrink. However, the CNTs remained unchanged. Thus, the direction of matrix shrinkage was hindered by the CNTs, thereby inhibiting the development of cracks.
- 2) Micro-filling: The small size of CNTs could refine the pores and improve the pore structure of the geopolymer.
- 3) Mechanical interlocking effect: By bridging both ends of the crack, additional work was required in case of failure. Thus, the rupture strength and flexural toughness of the geopolymer were improved.

Based on a study on the microstructure of geopolymers strengthened by PVA fibres, it was found that PVA fibres had little effect on crack resistance and pore-filling. The main benefit of PVA fibres is that they can be evenly distributed in the geopolymer matrix. Furthermore, it can change the stress distribution of the geopolymer matrix, improve the toughness of the geopolymer via mechanical interlocking, improve the mechanical properties of the geopolymer, and change the failure mode of the geopolymer in compression tests.

When PVA fibres and CNTs were mixed to strengthen the geopolymer, the two types of fibre-strengthened geopolymers, from macro and micro perspectives, complemented each other to

improve the mechanical properties and compressive failure mode of the geopolymer. A multi-scale dual-fibre strengthening mechanism was proposed (Figure 11) in this study. The geopolymer strengthened with PVA fibres and CNTs shrinks in the consolidation hardening stage. Owing to the presence of CNTs, the development of micropores and microcracks was limited. Furthermore, CNTs are involved in micro-filling, which refines the microstructure of the geopolymer. At this stage, a small number of CNT active groups participated in the reaction of the geopolymer, forming a firm bond. When the strengthened geopolymer matrix was subjected to an external force, the original micropores and microcracks in the system began to expand. During this time, CNTs which bridged both ends of the micropores and microcracks or filled the micropores were subjected to the gradually increasing external force. The phenomena of CNTs breaking and pulling-out appeared gradually, which indicated the additional work needed for crack propagation. When the external force continued to increase, the microcracks that were deflected, bifurcated, or shielded by the bridging effect of CNTs continued to develop. At this time, the load was transferred to the PVA fibres that were evenly distributed in the geopolymer matrix. Thus, the cracks were bifurcated, deflected, or limited. With an increase in the external force, PVA fibres exhibited pull-out, breakage, and other phenomena before failing. The cracks continued to develop until the system was destroyed.

CONCLUSION

In this study, the strengthening mechanism of PVA fibre and CNT-strengthened geopolymer were analysed. Additionally, a multi-scale dual-fibre strengthening mechanism was proposed in this study. The experimental results and discussion led to the following conclusions:

- 1) PVA fibres and CNTs have a good effect on improving the mechanical properties and microstructure of the geopolymer.

REFERENCES

- Bonapasta, A. A., Buda, F., Colombet, P., and Guerrini, G. (2002). Cross-Linking of Poly(Vinyl Alcohol) Chains by Ca Ions in Macro-defect-free Cements. *Chem. Mater.* 14, 1016–1022. doi:10.1021/cm010573q
- Carriço, A., Bogas, J. A., Hawreen, A., and Guedes, M. (2018). Durability of Multi-Walled Carbon Nanotube Reinforced concrete. *Construction Building Mater.* 164, 121–133. doi:10.1016/j.conbuildmat.2017.12.221
- China National Standards (2009). *Standard for Test Method of Basic Properties of Construction Mortar*. Shanxi: Shanxi Academy of Architectural Sciences JGJ/T70-2009.
- Davidovits, J. (1994a). “Alkaline Cements and Coneretes,” in Proceedings First International Confereneon Alkaline Cements and Coneretes KIEV, Ukraine, 1–19.
- Davidovits, J., Comrie, D. C., Paterson, J. H., and Ritcey, D. J. (1990). Geopolymeric Concretes for Environmental Protection. *C.I.* 12 (7), 30–40.
- Davidovits, J., Fernández-Jiménez, A., Provis, J. L., Lukey, G. C., Palomo, A., and van Deventer, J. S. J. (1998). Geopolymers and Geopolymeric Materials. *J. Therm. Anal.* 35, 429–441. doi:10.1007/BF01904446

Moreover, the incorporation of PVA fibres can improve the damage morphology of the geopolymer.

- 2) The effects caused by adding PVA fibres to the geopolymer are mainly physical. The toughness and the failure mode of the geopolymer improves owing to fibre pull-out, fibre breakage, fibre debonding, change in the internal stress distribution of the geopolymer.
- 3) The effects caused by adding CNTs to the geopolymer are chemical and physical in nature. The chemical strengthening effect is manifested by a small amount of CNTs participating in the geopolymer reaction to form a strong bond. The physical strengthening effect involve crack resistance, filling effect, and mechanical interlocking effect.
- 4) The blending of PVA fibres and CNTs has a good hybrid effect that can maximize the strengths and avoid weaknesses while playing a role in improving the mechanical properties, microstructure, and damage morphology of the geopolymer. However, an optimal blending amount is existed.

DATA AVAILABILITY STATEMENT

The original contributions presented in the study are included in the article/supplementary material, further inquiries can be directed to the corresponding author.

AUTHOR CONTRIBUTIONS

TM designed the experiments, analyzed data and wrote a part of the manuscript. XY wrote the manuscript and revised it. YY and HY performed the experimental work and MH revised the manuscript.

FUNDING

The authors are thankful for the financial support from the National Natural Science Foundation of China (52078453).

- Davidovits, J. (1979). *Polymère Minéral*. FR. Patent No FR 2,464,227. French Patent Application FR 79.22041.
- Davidovits, J. (1994b). “Properties of Geopolymer Cements,” in Proceedings First International Confereneon Alkaline Cements and Coneretes KIEV, Ukraine, 131–149.
- Duxson, P. (2007). Geopolymer Technology: the Current State of the Art. *J. Mater. Sci.* 42, 2917–2933. doi:10.1007/s10853-006-0637-z
- Davidovits, J. (2013). Geopolymer Cement: A Review. Geopolymer Institute Library. Available at: (Accessed December 1, 2020).
- Hamzaoui, R., Guessasma, S., Mecheri, B., Eshtiagh, A. M., and Bennabi, A. (2014). Microstructure and Mechanical Performance of Modified Mortar Using Hemp Fibres and Carbon Nanotubes. *Mater. Des. (1980-2015)* 56, 60–68. doi:10.1016/j.matdes.2013.10.084
- He, P., Jia, D., Zheng, B., Yan, S., YuanYang, J. Z., Yang, Z., et al. (2016). SiC Fiber Reinforced Geopolymer Composites, Part 2: Continuous SiC Fiber. *Ceramics Int.* 42 (10), 12239–12245. doi:10.1016/j.ceramint.2016.04.168
- Iijima, S. (1991). Helical Microtubules of Graphitic Carbon. *Nature* 354 (6348), 56–58. doi:10.1038/354056a0
- Khan, M. Z. H., Hao, Y., Hao, H., and Shaikh, F. U. A. (2018). Experimental Evaluation of Quasi-Static and Dynamic Compressive Properties of Ambient-

- Cured High-Strength plain and Fiber Reinforced Geopolymer Composites. *Construction Building Mater.* 166, 482–499. doi:10.1016/j.conbuildmat.2018.01.166
- Khater, H. M., and Abd el Gawaad, H. A. (2016). Characterization of Alkali Activated Geopolymer Mortar Doped with MWCNT. *Construction Building Mater.* 102, 329–337. doi:10.12989/amr.2015.4.1.45
- Kong, D. L. Y., Sanjayan, J. G., and Sagoe-Crentsil, K. (2007). Comparative Performance of Geopolymers Made with Metakaolin and Fly Ash after Exposure to Elevated Temperatures. *Cement Concrete Res.* 37 (12), 1583–1589. doi:10.1016/j.cemconres.2007.08.021
- Kusak, I., Lunak, M., and Rovnanik, P. (2016). Electric Conductivity Changes in Geopolymer Samples with Added Carbon Nanotubes. *Proced. Eng.* 151, 157–161. doi:10.1016/j.proeng.2016.07.361
- Li, Z., Zhang, J., and Wang, M., (2020). Structure, Reactivity, and Mechanical Properties of Sustainable Geopolymer Material: A Reactive Molecular Dynamics Study. *Front. Mater.* 7, 1–13. doi:10.3389/fmats.2020.00069
- Liebscher, M., Fuge, R., Schröfl, C., Lange, A., Caspari, A., Bellmann, C., et al. (2017). Temperature- and pH-dependent Dispersion of Highly Purified Multiwalled Carbon Nanotubes Using Polycarboxylate-Based Surfactants in Aqueous Suspension. *J. Phys. Chem. C* 121, 16903–16910. doi:10.1021/acs.jpcc.7b05534
- Lizcano, M., Kim, H. S., Basu, S., and Radovic, M., (2012). Mechanical Properties of Sodium and Potassium Activated Metakaolin-Based Geopolymers. *J. Mater. Sci.* 47, 2607–2616. doi:10.1007/s10853-011-6085-4
- Nematollahi, B., Qiu, J., Yang, E. H., and Sanjayan, J. G.. (2017). Microscale Investigation of Fiber-Matrix Interface Properties of Strain-Hardening Geopolymer Composite. *Ceram. Int.* 43, 15616–15625. doi:10.1016/j.ceramint.2017.08.118
- Nematollahi, B., Xia, M., and Sanjayan, J. (2019). Post-processing Methods to Improve Strength of Particle-Bed 3D Printed Geopolymer for Digital Construction Applications. *Front. Mater.* 6, 1–10. doi:10.3389/fmats.2019.00160
- Pelisser, F., Guerrino, E. L., Menger, M., Michel, M. D., and Labrincha, J. A. (2013). Micromechanical Characterization of Metakaolin-Based Geopolymers. *Construction Building Mater.* 49, 547–553. doi:10.1016/j.conbuildmat.2013.08.081
- Purdon, A. O. (1940). The Action of Alkalis on Blast-Furnace Slag. *J. Soc. Chem. Ind.* 59, 191–202.
- Rovnanik, P., Šimonová, H., Topolář, L., Bayer, P., Schmid, P., and Keršner, Z. (2016b). Carbon Nanotube Reinforced Alkali-Activated Slag Mortars. *Construction Building Mater.* 119, 223–229. doi:10.1016/j.conbuildmat.2016.05.051
- Rovnanik, P., Šimonová, H., Topolář, L., Schmid, P., and Keršner, Z. (2016a). Effect of Carbon Nanotubes on the Mechanical Fracture Properties of Fly Ash Geopolymer. *Proced. Eng.* 151, 321–328. doi:10.1016/j.proeng.2016.07.360
- Ruoff, R. S., and Lorents, D. C. (1995). Mechanical and thermal Properties of Carbon Nanotubes. *Carbon* 33 (7), 925–930. doi:10.1016/0008-6223(95)00021-5
- Sá Ribeiro, R. A., Sá Ribeiro, M. G., and Kriven, W. M. (2017). A Review of Particle- and Fiber-Reinforced Metakaolin-Based Geopolymer Composites. *J. Ceram. Sci. Technol.* 8 (3), 307–322. doi:10.4416/JCST2017-00048
- Saafi, M., Andrew, K., Tang, P. L., Mcghon, D., Taylor, S., Rahman, M., et al. (2013). Multifunctional Properties of Carbon Nanotube/fly Ash Geopolymeric Nanocomposites. *Construction Building Mater.* 49 (12), 46–55. doi:10.1016/j.conbuildmat.2013.08.007
- Shi, Y., Zhang, Z., Sang, Z., and Zhao, Q. (2020). Microstructure and Composition of Red Mud-Fly Ash-Based Geopolymers Incorporating Carbide Slag. *Front. Mater.* 7, 1–11. doi:10.3389/fmats.2020.563233
- Sukontasukkul, P., Pongsopha, P., Chindaprasit, P., and Songpiriyakij, S. (2018). Flexural Performance and Toughness of Hybrid Steel and Polypropylene Fibre Reinforced Geopolymer. *Construction Building Mater.* 161, 37–44. doi:10.1016/j.conbuildmat.2017.11.122
- Wu, X. J., and Zhang, S. S. (2017). The Influence of Defoamer on the Compactness of Ultra -lightweight Cement Composite. *Eng. Res.* 49 (6), 1–4. doi:10.13402/j.gcjs.2017.06.001
- Yang, T., Han, E., Wang, X., and Wu, D. (2017). Surface Decoration of Polyimide Fiber with Carbon Nanotubes and its Application for Mechanical Enhancement of Phosphoric Acid-Based Geopolymers. *Appl. Surf. Sci.* 416, 200–212. doi:10.1016/j.apsusc.2017.04.166
- Yang, Y. H., and Li, W. Z. (2011). Radial Elasticity of Single-Walled Carbon Nanotube Measured by Atomic Force Microscopy. *Appl. Phys. Lett.* 98 (4), 041901. doi:10.1063/1.3546170
- Yasari, S., Hajiaghahi, G., Mohammadi, F., Mahdikhani, M., and Farokhzad, R. (2017). The Role of Synthesis Parameters on the Workability, Setting and Strength Properties of Binary Binder Based Geopolymer Paste. *Construction Building Mater.* 157, 534–545. doi:10.1016/j.conbuildmat.2017.09.102
- Yu, M.-F., Kowalewski, T., and Ruoff, R. S. (2000a). Investigation of the Radial Deformability of Individual Carbon Nanotubes under Controlled Indentation Force. *Phys. Rev. Lett.* 85 (7), 1456–1459. doi:10.1103/PhysRevLett.85.1456
- Yu, M.-F., Lourie, O., Dyer, M. J., Moloni, K., Kelly, T. F., and Ruoff, R. S. (2000b). Strength and Breaking Mechanism of Multiwalled Carbon Nanotubes under Tensile Load. *Science* 287 (5453), 637–640. doi:10.1126/science.287.5453.637
- Yuan, J., He, P., Jia, D., Fu, S., Zhang, Y., Liu, X., et al. (2017). *In Situ* processing of MWCNTs/leucite Composites through Geopolymer Precursor. *J. Eur. Ceram. Soc.* 37 (5), 2219–2226. doi:10.1016/j.jeurceramsoc.2017.01.008
- Yuan, J., He, P., JiaLanlan, D. X., Yan, S., Cai, D., Xu, L., et al. (2016). SiC Fiber Reinforced Geopolymer Composites, Part 1: Short SiC Fiber. *Ceramics Int.* 42 (4), 5345–5352. doi:10.1016/j.ceramint.2015.12.067
- Zhang, P., Kang, L. Y., Wei, H., and Yang, Y. H. (2019). Effect of PVA Fiber and Nano-SiO₂ on Fracture Properties of Geopolymer Mortar. *J. Build. Mater.* 22 (6), 986–992. doi:10.3969/j.issn.1007-9629.2019.06.022
- Zhang, Q., and Yang, P. (2001). A Study on the Microstructures of Clay Minerals and Deflocculants Selected in Ceramics Processing. *China Ceram.* (5), 30–31. doi:10.16521/j.cnki.issn.1001-9642.2001.05.010

Conflict of Interest: Author YY was employed by the company Urban Planning and Architectural Design Institute of Fudan University Co., Ltd. Author HY was employed by the company Hangzhou Xincheng Dinghong Real Estate Development Co., Ltd. Author MH was employed by the company Wenzhou Design Assembly Company Ltd.

The remaining authors declare that the research was conducted in the absence of any commercial or financial relationships that could be construed as a potential conflict of interest.

Publisher's Note: All claims expressed in this article are solely those of the authors and do not necessarily represent those of their affiliated organizations, or those of the publisher, the editors and the reviewers. Any product that may be evaluated in this article, or claim that may be made by its manufacturer, is not guaranteed or endorsed by the publisher.

Copyright © 2021 Meng, Yang, Yu, Yu and Huang. This is an open-access article distributed under the terms of the Creative Commons Attribution License (CC BY). The use, distribution or reproduction in other forums is permitted, provided the original author(s) and the copyright owner(s) are credited and that the original publication in this journal is cited, in accordance with accepted academic practice. No use, distribution or reproduction is permitted which does not comply with these terms.